Inorganic Chemistry

Article

pubs.acs.org/IC

In Situ Construction of Three Anion-Dependent Cu(I) Coordination Networks as Promising Heterogeneous Catalysts for Azide−Alkyne "Click" Reactions

Zhenghu Xu,[†] Lu−Lu Han,[†] Gui−Lin Zhuang,[‡] Jing Bai,[†] and Di Sun*[,†]

[†]Key Lab of Colloid and Interface Chemistry, Ministry of Education, School of Chemistry and Chemical Engineering, Shandong University, Jinan, 250100, P. R. China

[‡]College of Chemical Engineering and Materials Science, Zhejiang University of Technology, Hangzhou, 310032, P. R. China

Supporting Information

ABSTRACT: Three Cu(I) coordination networks, namely, $\{[Cu_2(bpz)_2(CN)X]\cdot CH_3CN\}_n$, (X = Cl, **1**; I, **3**), $\{[Cu_6(bpz)_6(CH_3CN)_3(CN)_3Br]\cdot 2OH\cdot 14CH_3CN\}_n$, (**2**, bpz = 3,3′,5,5′-tetramethyl-4,4′-bipyrazole), were prepared by using solvothermal method. The cyanide ligands in these networks were generated in situ by cleavage of C−C bond of MeCN under solvothermal condition. The structures of these networks are dependent on halogen anions. Complex **1** is a ladderlike structure with μ_2-CN^- as rung and μ_2-bpz as armrest. The Cl^- in **1** is at terminal position but does not extend the one-dimensional (1D) ladder to higher dimensionalities. Complex **2** is a three-dimensional (3D) framework comprised of novel planar $[Cu_3Br]$ triangle and single Cu nodes, which are extended by μ_2-bpz and μ_2-CN^- to form a novel (3,9)-connected **gfy** network. Density functional theory calculations showed that single-electron delocalization of Br atom induces the plane structure of $[Cu_3Br]$. Complex **3** also possesses a similar ladderlike subunit as in **1**, but the I^- acts as bidentate bridge to extend the ladder to 3D framework with a four-connected **sra** topology. The three networks show notable catalytic activity on the click reaction. The compared catalytic results demonstrate that complex **2** possesses the best catalysis performance among three complexes, which is ascribed to the largest solvent-accessible void (porosity: **2** (29.4%) > **1** (25.7%) > **3** (17.6%)) and the more Cu(I) active sites in **2**. The present combined structure−property studies provide not only a new synthetic route to obtain a new kind of catalyst for click reaction but also the new insights on catalyst structure−function relationships.

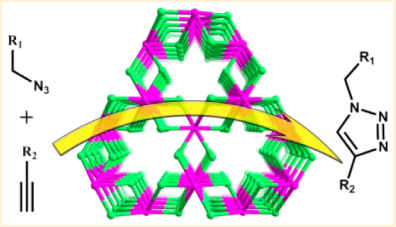

INTRODUCTION

In recent years, a new class of inorganic−organic hybrid crystalline materials constructed from inorganic metal nodes and organic linkers have attracted considerable interest. Because of their structural aesthetics, diversity, and modulability, these crystalline materials can potentially be applied in photoluminescence, magnetism, conductivity, nonlinear optics, gas storage, chemical sensing, catalysis, and drug delivery.[1] The final coordination networks formed by coordination bonding interaction by using inorganic and organic component can be structurally modulated by various factors such as metal−ligand ratio, counter-anions, and solvents.[2] By modulating the structures, the functionalities of the networks can be realized. On the other hand, in situ reaction in one-pot assembly under the solvothermal condition usually gives unexpected results.[3] For example, the solvothermal in situ generation of CN^- from nitriles offers a new approach to produce fascinating metal-cyanide coordination networks, which were not available by cyanometalates as the source.[4] However, up to now, cyanide-containing coordination networks in situ obtained from solvothermal reaction have been reported sporadically.[5]

As we know, the photoluminescence, magnetism, and gas storage properties of coordination networks have been investigated most intensively, whereas catalysis based on coordination networks is still an underdeveloped areas.[6] This is partly because their structures are not stable enough in the catalytic reactions. Accessible active site is another prerequisite by using coordination networks as catalysts, but the permanent porosity of a metal−organic framework (MOF) is usually difficult to maintain once they are activated by excluding the solvents.[7] Since the pioneering work of Fokin, Sharpless, and Meldal,[8] a large variety of Cu(I) and Cu(II) catalysts for the azide−alkyne cycloaddition (CuAAC) have been developed.[9] Corma et al. used cagelike $Cu^{II}(pymo)_2$ (pymo = 2-hydroxypyrimidinolate)[10a] as recycled heterogeneous catalyst to realize the click reaction.[10b] In their work, $Cu^{II}(pymo)_2$ worked as a precatalyst, which is in situ reduced to catalytically active Cu(I) species by alkynes, as for instance in the well-known Glaser coupling.[11] Although the gradual maturation of crystal engineering has pushed large progress in coordination network catalysis,[12] only very few works have been reported by directly using CuX (X = Cl, Br, I) coordination networks as heterogeneous catalysts for the click reaction. Yet to be demonstrated is catalytic chemistry that fully exploits the

Received: January 16, 2015
Published: May 5, 2015

DOI: 10.1021/acs.inorgchem.5b00110
Inorg. Chem. 2015, 54, 4737−4743

Table 1. Crystal Data Collection and Structure Refinement for 1−3

compound	1	2	3
empirical formula	$C_{23}H_{31}ClCu_2N_{10}$	$C_{73}H_{99}BrCu_6N_{32}$	$C_{23}H_{31}Cu_2IN_{10}$
M_r	610.11	1885.99	701.56
temperature/K	298(2)	200(2)	298(2)
crystal system	orthorhombic	hexagonal	orthorhombic
space group	*Pnam*	$P6_3/m$	*Pnam*
a/Å	12.698(3)	19.003(5)	11.406(5)
b/Å	14.273(4)	19.003(5)	14.981(7)
c/Å	17.008(4)	16.916(5)	16.867(8)
α/deg	90.00	90.00	90.00
β/deg	90.00	90.00	90.00
γ/deg	90.00	120.00	90.00
volume/Å^3	3082.4(14)	5290(2)	2882(2)
Z	4	2	4
ρ_{calc} g/cm^3	1.315	1.184	1.617
μ/mm^{-1}	1.495	1.611	2.577
$F(000)$	1256.0	1940.0	1400.0
reflns collected	14397	20357	13422
R_{int}	0.1026	0.1177	0.0456
independent reflns	2807	3214	2619
parameters	179	184	179
goodness of fit	0.981	0.983	1.050
R_1/wR_2 $[I \geq 2\sigma(I)]^{a,b}$	0.0758/0.2085	0.0634/0.1565	0.0332/0.0819
R_1/wR_2 [all data]^{a,b}	0.1308/0.2572	0.1156/0.1756	0.0474/0.0895
largest residuals e Å^{-3}	0.932/−0.723	0.455/−0.612	0.697/−0.640

$^aR_1 = \sum| |F_o| - |F_c| |/\sum|F_o|$. $^bwR_2 = [\sum w(F_o^2 - F_c^2)^2]/\sum w(F_o^2)^2]^{1/2}$.

structural features of coordination networks to accomplish unique catalysis performance.

On the basis of these considerations, herein we present three CuX coordination networks, namely, $\{[Cu_2(bpz)_2(CN)X]\cdot CH_3CN\}_n$, (X = Cl, **1** and I, **3**) and $[Cu_6(bpz)_6(CH_3CN)_3(CN)_3Br\cdot 14CH_3CN\cdot 2OH]_n$, (**2**, bpz = 3,3′,5,5′-tetramethyl-4,4′-bipyrazole), which exhibit interesting one-dimensional (1D) ladder, three-dimensional (3D) (3,9)-connected **gfy** network and 3D 4-connected **sra** network, respectively. Interestingly, in situ generated cyanide group from the cleavage of a carbon−carbon bond of acetonitrile was observed, and the controlling feature of the synthesis is the halogen anion chosen. Three complexes are efficient catalysts for the click reactions. The catalyst can be recycled after the reactions by simple decantation and reused without significant degradation in catalytic activity. This is the first example of the application of CuX coordination networks in click reactions. The correlation between catalytic activity and structures is also elucidated.

EXPERIMENTAL SECTION

Materials and General Methods. All chemicals and solvents used in the syntheses were of analytical grade and used without further purification. IR spectra were recorded on a Nicolet AVATAT FT-IR360 spectrometer as KBr pellets in the frequency range of 4000−400 cm^{-1}. All ^{1}H NMR spectra were recorded on Bruker-300 MHz spectrometer. The elemental analyses (C, H, N content) were determined on a Vario EL III analyzer. Powder X-ray diffraction (PXRD) data were collected on a Philips X'Pert Pro MPD X-ray diffractometer with Cu Kα radiation equipped with an X'Celerator detector. Thermogravimetric analyses (TGA) were performed on a Netzsch STA 449C thermal analyzer from room temperature to 800 °C under nitrogen atmosphere at a heating rate of 10 °C/min. Electron paramagnetic resonance (EPR) spectra of solid samples were recorded on a Bruker X-band EPR spectrometer equipped with a temperature controller. The quantification of leached Cu(II) ion after catalysis were performed by a Leaman inductively coupled plasma mass spectrometry (ICP-MS) spectrometer.

Synthesis of $\{[Cu_2(bpz)_2(CN)Cl]\cdot CH_3CN\}_n$ (1). A mixture of CuCl (10.0 mg, 0.1 mmol) and bpz (19.0 mg, 0.1 mmol) in CH_3CN-H_2O (5 mL, 1:1 v/v) was heated to 160 °C in 8 h in a 25 mL Teflon-lined reaction vessel, kept at 160 °C for 33 h, and then slowly cooled to 30 °C in 13 h. Colorless rodlike crystals of **1** were isolated by filtration, washed with H_2O, and dried in air. Anal. Calcd (%) for **1** ($C_{23}H_{31}ClCu_2N_{10}$) C 45.28, H 5.12, N 22.96; found C 45.11, H 5.75, N 22.45. Selected IR peaks (cm^{-1}): 3304(s), 3089(w), 2923(w), 2079(s), 1567(w), 1298(w), 1254(w), 1027(m), 668(m), 587(m).

Synthesis of $\{[Cu_6(bpz)_6(CH_3CN)_3(CN)_3Br]\cdot 2OH\cdot 14CH_3CN\}_n$ (2). Synthesis of **2** is similar to that of **1** but using CuBr (14.3 mg, 0.1 mmol) instead of CuCl (10 mg, 0.1 mmol). Colorless needlelike crystals of **2** were isolated by filtration, washed with H_2O, and dried in air. Anal. Calcd (%) for **2** ($C_{89}H_{125}BrCu_6N_{40}O_2$) C 45.64, H 5.41, N 29.63; found C 45.78, H 5.26, N 29.92. Selected IR peaks (cm^{-1}): 3341(s), 2922(w), 2108(w), 1420(m), 1306(w), 1163(w), 1026(s), 667(m).

Synthesis of $\{[Cu_2(bpz)_2(CN)I]\cdot CH_3CN\}_n$ (3). Synthesis of **3** is similar to that of **1** but using CuI (19.0 mg, 0.1 mmol) instead of CuCl (10 mg, 0.1 mmol). Yellow block crystals of **3** were isolated by filtration, washed with H_2O, and dried in air. Anal. Calcd (%) for **3** ($C_{23}H_{31}Cu_2IN_{10}$) C 39.38, H 4.45, N 19.97, found C 40.05, H 4.68, N 19.55. Selected IR peaks (cm^{-1}): 3336(s), 2918(w), 2090(w), 1562(w), 1309(w), 1024(m), 665(m), 589(m).

Computational Details. All calculations were performed in Gaussian 03 software. Geometry optimization and single-point calculation were accomplished by using the spin-polarized density functional theory (DFT) with B3LYP hybrid functional. C, H, N, and Br atoms employed the basic set level of 6-31G*. For three Cu atoms, the pseudo basic set of LANL2DZ was applied. Natural orbital analysis was performed by using of NBO Version 3.1 of Gaussian package.

Catalytic Studies. In a typical experiment, to a Schlenk tube was added solid MOF catalyst **2** (3.2 mg, 0.01 mmol, 1 mol %). Then dimethylformamide (DMF, 0.5 mL) and dimethyl sulfoxide (DMSO, 0.5 mL), **4a** (133 mg, 1 mmol), and **5a** (102 mg, 1 mmol) were all added to the reaction system. The resulting mixture was stirred under

DOI: 10.1021/acs.inorgchem.5b00110
Inorg. Chem. 2015, 54, 4737−4743

nitrogen atmosphere at 60 °C for 4 h. The reaction mixture was filtered, and the catalyst was recovered. The filtrate was diluted with dichloromethane and washed with water. The organic phase was evaporated under reduced pressure and purified by a short column chromatography (silica gel) to afford the pure product **6a** (233 mg) in 99% yield.

RESULTS AND DISCUSSION

Synthesis and General Characterization. Solvothermal reaction of CuX (X = Cl, **1**; Br, **2**; I, **3**) with bpz in acetonitrile−H_2O (1:1 v/v) at 160 °C yielded colorless crystals of **1** and **2** and yellow crystals of **3**. All products were isolated as fine crystals, and some well-defined single crystals could be picked for X-ray diffraction analysis (Table 1). The in situ generated cyanide ligands were derived from the cleavage of C−C bond of acetonitrile in solvothermal condition. Phase purity of **1**−**3** is sustained by its PXRD pattern, which is consistent with that simulated on the basis of the single-crystal X-ray diffraction data (Figure S1 in the Supporting Information). The differences in intensity may be due to the preferred orientation of the crystalline powder samples. The TGA for **1**−**3** is measured under the N_2 atmosphere (Supporting Information, Figure S2). For **1**, the weight loss of 5.95% in the temperature range from 30 to 100 °C is attributed to the removal of CH_3CN molecules (calcd 6.73%). The solvent-free framework starts to decompose at 155 °C by losing the organic ligand. Complex **2** loses free CH_3CN molecules from 30 to 190 °C (found 22.95%, calcd 23.82%). Complex **3** loses free CH_3CN molecules from 130 to 180 °C (found 5.50%, calcd 5.85%). IR spectra (Supporting Information, Figure S3) of **1**−**3** show ν_{CN} at 2082, 2110, and 2095 cm^{-1}, respectively, indicating the existence of μ-CN^-. These results agree well with crystal structures of **1**−**3**.

Crystal Structure of $\{[Cu_2(bpz)_2(CN)Cl]\cdot CH_3CN\}_n$ (1). Single-crystal X-ray structural analysis of **1** reveals that it crystallizes in orthorhombic *Pnam* space group and that its asymmetric unit contains two halves Cu(I) atoms, one bpz ligand, a half of Cl^-, a half of CN^-, and a half of guest acetonitrile molecule. Notably, two unique Cu(I) atoms, Cl^-, and CN^- are bisected by a crystallographic mirror perpendicular to [0,0,1], giving them half occupancy. The Cu1 atom locates in a slightly distorted tetrahedral coordination environment (τ_4 value is 0.90),[13] completed by two N atoms from two different bpz ligands, one N atom of CN^- ion, and one terminal Cl^- ion, whereas Cu2 is coordinated by two N atoms of bpz and one C atom of CN^- ion, forming a nearly planar triangular geometry (Figure 1a). The average bond angle around Cu2 is 117.3°. The Cu−N, Cu−C, and Cu−Cl bond lengths (Cu−N = 1.952(13)−2.022(6) Å; Cu−C = 1.855(12) Å; Cu−Cl = 2.417(4) Å) are comparable with similar complexes.[14] Each bpz and CN^- ion are bidentate bridges and extend the Cu(I) atoms to form a 1D ladder structure running along *c* axis, where μ_2-CN^- as rung and μ_2-bpz as armrest (Figure 1b). The solvent-accessible volume for **1** is estimated to be ca. 25.7% by removal of the free CH_3CN molecules. The 1D channel generated by the interconnection of irregular cavities is found in **1** with the maximum diameter of 2.41 Å.

Crystal Structure of $\{[Cu_6(bpz)_6(CH_3CN)_3(CN)_3Br]\cdot 2OH\cdot 14CH_3CN\}_n$ (2). Complex **2** crystallizes in the hexagonal space group $P6_3/m$ and features a 3D (3,9)-connected **gfy** network. Its asymmetric unit consists of two halves Cu(I) atoms, one bpz ligand, one-sixth of Br^-, a half of CN^-, and a half of coordinated acetonitrile molecule. Notably, two unique Cu(I) atoms,

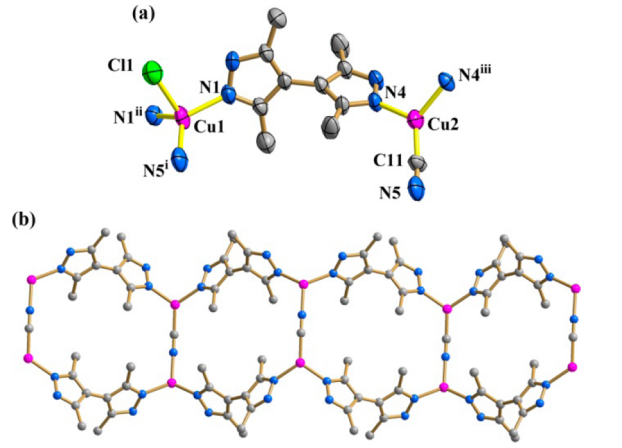

Figure 1. (a) ORTEP representation of **1** showing the local coordination environments around Cu(I) center with 50% thermal ellipsoid probability. (Symmetry codes: (i) $-x + 2, -y + 1, -z + 1$; (ii) $x, y, -z + 3/2$; (iii) $x, y, -z + 1/2$). (b) Ball-and-stick view of the 1D ladder, terminal Cl ligand was removed for clarity. (Cu: purple, C: gray, N: blue).

coordinated acetonitrile molecule, and CN^- are bisected by a crystallographic mirror perpendicular to [0,0,1], giving them half occupancy. For Br^-, the same mirror bisects it, and a sixfold axis passes through it, giving it site occupancy of 1/6. As shown in Figure 2a, both Cu1 and Cu2 atoms are in slightly distorted tetrahedral coordination geometry with τ_4 values of 0.92 and 0.95, respectively. Cu1 is coordinated by two N atoms from two different bpz ligands, one N atom of CN^- ion, and one Br^- ion,

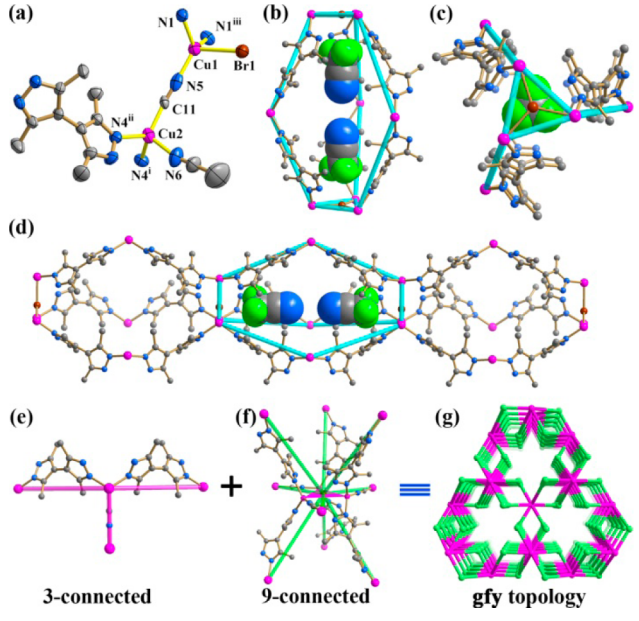

Figure 2. (a) ORTEP representation of **2** showing the local coordination environments around Cu(I) center with 50% thermal ellipsoid probability. (symmetry codes: (i) $-x + 1, -y + 1, z + 1/2$; (ii) $-x + 1, -y + 1, -z + 1$; (iii) $x, y, -z + 3/2$) (b) and (c) Ball-and-stick view of the shuttlelike C_{6h} $[Cu_9(bpz)_6]$ cage encapsulating a pair CH_3CN molecules viewed along two different directions. (Cu: purple, C: gray; N: blue; Br: brown; H: green). (d) The propagation of the cages by sharing the $[Cu_3Br]$ plane. (e) 3-connected Cu2 node. (f) 9-connected $[Cu_3Br]$ subunit. (g) Schematic representation of simplified 3D network with **gfy** topology.

DOI: 10.1021/acs.inorgchem.5b00110
Inorg. Chem. 2015, 54, 4737−4743

whereas Cu2 is coordinated by two N atoms of bpz, one N atom of acetonitrile molecule, and one C atom of CN^- ion (Cu−N = 1.918(10)−2.057(10) Å; Cu−C=1.868(9) Å). Three equatorial Cu(I) ions form an equilateral triangle assisted by a central μ_3-Br-bridging ion and three peripheral μ_2-CN ions. The Br^- ion locates exactly in the center of the Cu3 triangle, exhibiting a uniform Br−Cu bond length of 2.6344 (12) Å. Three CN^- anions are also coplanar to the Cu3 triangle plane. The resulting $[Cu_3Br]$ triangle is linked to single Cu2 node by bidentate bpz ligands to generate a shuttlelike C_{6h} $[Cu_9(bpz)_6]$ cage (Figure 2b,c). A pair of symmetry-related CH_3CN molecules was encapsulated in each cage by Van der waals interaction. The cages propagate along the *c* axis by sharing the $[Cu_3Br]$ plane (Figure 2d) and then are extended by μ_2-CN^- to generate the final 3D framework (Supporting Information, Figure S4). Topologically, each $[Cu_3Br]$ subunit is linked to nine Cu2 centers by three CN^- anions and six bpz ligands, whereas each Cu2 single node is linked to three $[Cu_3Br]$ subunit by one CN^- anion and two bpz ligands; as a result, the $[Cu_3Br]$ subunit and Cu2 center could be seen as a 9- and 3-connected node, respectively (Figure 2e and 2f). The overall topological structure of **2** possesses a binodal (3,9)-connected **gfy** topology (Figure 2g) with a Schläfli symbol of $\{4^3\}_3\{4^{12}\cdot6^{15}\cdot8^9\}$ as calculated by TOPOS program.[15] Although some coordination networks with (3,9)-connected topology have been constructed,[16] to our knowledge, only two examples with **gfy** topology, namely, MIL-110 and $[Cu_7I_4]$ cluster-based network,[17] were reported until now. The solvent-accessible volume for **2** is estimated to be ca. 29.4% by removal of the free CH_3CN molecules. The void space of **2** consists of both 1D channels and closed cavities with the maximum diameter of 3.40 Å.

Quantum Chemical and Experimental Investigations on the Planar $[Cu_3Br]$ Triangle in 2. The planar tricoordinate Br is an unusual motif in Cu(I) chemistry. For Cu(I) coordination complexes, Br is typically out of the plane of the three metal centers, whereas the $[Cu_3Br]$ subunit core is perfectly planar in **2** imposed by crystallographic symmetry elements. No precedents containing this motif could be found in the Cambridge Structure Database (Version 5.35, Feb. 2014),[18] and the only related complexes are an octanuclear Cd(II) cage templated by a pair of planar μ_3-Br ions,[19a] a triple-stranded octanuclear Cd(II) helicate,[19b] and trinuclear Fe(II) or Mn(II) complex supported by cyclophane bearing three *β*-diketimine arms.[19c] To explain and understand such novel structural property of $[Cu_3Br]$ moiety, spin-polarized DFT calculations were conducted by help of Gaussian 03 program.[20] In this regard, the initial structure adopts $[Cu_3Br(CN)_3(pyrazole)_6]$ cluster model, where pyrazole molecule features same chemical characteristic (e.g., coordination atoms) with ligand. Full geometry optimization was first performed and reveals that resulting structure is good agreement with that of **2**. Frontier molecular orbitals were further calculated. As shown in Figure 3, these singly occupied molecular orbitals (SOMO) almost concentrate on 4p orbitals of Br, on 3d orbitals of Cu, and on 2p orbitals of pyrazole or CN^- ligands. Among them, bonding MO exists between 3d orbital ($3d_{xz}$ or $3d_{yz}$) of Cu and $4p_x$ or $4p_y$ orbital of Br in the 173*α* and 172*β* SOMOs, while there are antibonding Cu−Br MOs in other SOMOs. As shown in Table 2, atomic charge population results exhibit that charges are distributed on $[Cu_3Br]$ moiety, and valence electrons of Br are indeed moved to empty orbitals of three Cu. Furthermore, natural bond orbital analysis[21] reveals that Br ion employs $sp^{2.87}$ hybridization. Although Br has not plane-characteristic sp^2 hybridization, the remaining localized p_z-type electrons can effectively delocalize to three Cu and pyrazole or CN^- ligands, which is intuitively verified from 172*α* SOMO. Moreover, Mulliken population results display that the spin densities of Cu1, Cu2, Cu3, and Br are 0.230, 0.224, 0.204, and 0.184, respectively. That implies that spin magnetic moments have transferred from Br atom to three Cu so as to reduce the tension between bonding electrons and lone-pair electrons of Br. In general, it is concluded that single-electron delocalization of Br atom induces the plane structure of $[Cu_3Br]$ moiety. The existence of single electron in $[Cu_3Br]$ triangle is also justified by the broad electron paramagnetic resonance (EPR) spectra (Figure 3g) with a g = 2.07.

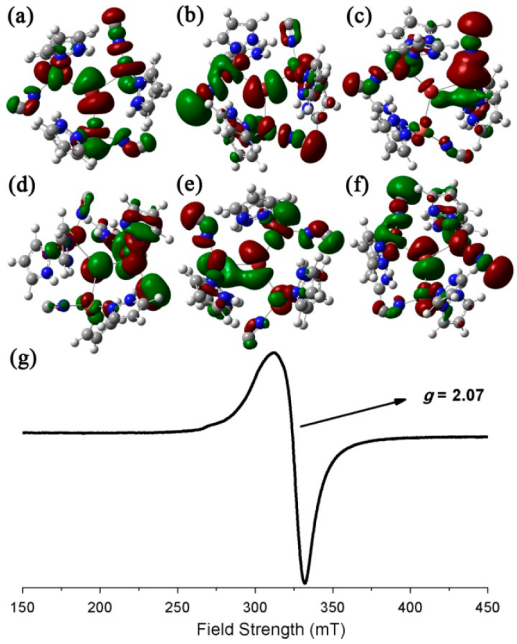

Figure 3. LUMO or 174*β* (a), HOMO or 174*α* (b), 173*α* (c), 172*α* (d), 172*β* (e), and 171*β* (f) of **2**. (g) Experimental EPR spectra of complex **2** obtained in solid state. Experimental conditions: microwave frequency, 9.397 GHz; microwave power, 2 mW; modulation frequency, 100 kHz.

Table 2. Atomic Charge Populations[a] of 2

method	Cu1	Cu2	Cu3	Br
Mulliken	0.285	0.279	0.275	−0.242
NBO	0.538	0.529	0.520	−0.305

[a]Unit: e.

Crystal Structure of $\{[Cu_2(bpz)_2(CN)I]\cdot CH_3CN\}_n$ (3). Complex **3** crystallizes in the same space group as **1** but features a 3D 4-connected **sra** network. The components in its asymmetric unit are identical with those in complex **1** except for the existence of μ_2-I^- instead of terminal Cl^- in **1**. As shown in Figure 4a, the coordination geometries of Cu1 and Cu2 are N3I and CN2I tetrahedra with τ_4 values of 0.93 and 0.92, respectively (Cu1−I1 = 2.7187 (12) Å and Cu2−I1 = 2.9872 (16) Å; ∠Cu1−I1−Cu2 = 110.43(4)°). In **3**, similar 1D ladder structural motif was also observed, but each ladder was further linked by μ_2-I^- to its four nearest ladders, forming the final 3D framework (Figure 4b). The Cl^- and I^- anions have different bonding ability and fashion toward Cu(I) atom, which causes the different structures for **1** and **3**. From the topological view,

DOI: 10.1021/acs.inorgchem.5b00110
Inorg. Chem. 2015, 54, 4737−4743

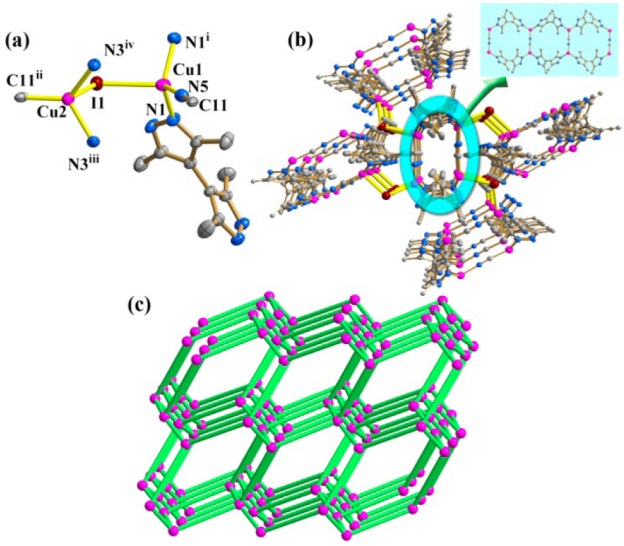

Figure 4. (a) ORTEP representation of **3** showing the local coordination environments around Cu(I) center with 50% thermal ellipsoid probability. ((i) $x, y, -z + 3/2$; (ii) $x + 1/2, -y + 3/2, -z + 3/2$; (iii) $-x + 1/2, y + 1/2, -z + 1$; (iv) $-x + 1/2, y + 1/2, z + 1/2$.) (b) Ball-and-stick view of the 3D framework showing the 1D ladder linked to its four neighbors. (Cu: purple, C: gray, N: blue, I: brown). (c) Schematic representation of simplified 3D network with **sra** topology.

the structure of **3** could be considered as being composed of Cu1 and Cu2 single metal nodes bridged by the organic ligand, I^- and CN^- ions; both the metal centers could be regarded as nodes. Each Cu(I) atom was bound to four neighbors acting as 4-connected node, and each ligand or anion connected to two Cu(I) atoms as 2-connected linker. In this way the structure could be reduced to a uninodal 4-connected **sra** (Schlafli symbol: $\{4^2 \cdot 6^3 \cdot 8\}$) topology network (Figure 4c). The solvent-accessible volume for **3** is estimated to be ca. 17.6% by removal of the free CH_3CN molecules. The pore shape of **3** is similar to that of **1**, and the maximum diameter for 1D channel is 2.44 Å.

Catalytic Activities toward the Azide–Alkyne Click Reaction. Copper-catalyzed azide–alkyne cycloaddition reaction (CuAAC), as a representative example of "click chemistry", have been recognized as the most attractive synthetic tools widely used in biochemistry and polymer chemistry.[22] In homogeneous catalysis, Cu(I) species directly used or reduced from Cu(II) are mostly used as the catalyst. However, a main limitation of this CuAAC reaction is the toxic copper residue in the products, which limited its practical use in biomolecules. To circumvent this problem the catalyst was immobilized on an organic polymer support or inorganic support such as silica, zeolite, and carbon.[23] Metal–organic framework (MOF) represents another very promising solid catalyst for a variety of organic reactions.[24] In Corma group's work of Cu(II)-MOFs catalyzed CuAAC reaction, the loading of copper catalyst was up to 10 mol %, and the Cu(II) species need to be in situ reduced to Cu(I) species[10] Thus, the direct use of Cu(I)-MOFs as catalysts is expected to be more efficient. However, to our surprise, this has not been reported so far.

Consideration of the catalytically active Cu(I) site and potential voids in **1**–**3**, catalytic activities of them toward the click reaction were tested (Table 3). At the outset, benzyl azide **4a** reacted with phenylacetylene **5a** in the presence of **3** (10 mol %) at 60 °C in DMF and DMSO solution. After 4 h, a very

Table 3. Cu(I)–MOF Catalyzed Azide–Alkyne Cycloaddition Reaction[a]

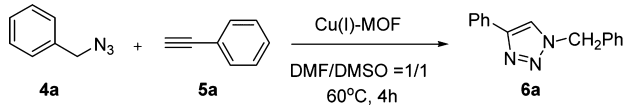

4a 5a 6a

entry	catalyst	yield[b] (%)
1	**3** (10 mol %)	99
2	**3** (1 mol %)	71
3	**2** (1 mol %)	99
4	**1** (1 mol %)	99

[a]Reaction conditions: benzyl azide **4a** (1 mmol), **5a** (1 mmol), Cu(I)-MOF catalyst (1 mol %, based on Cu element), DMF (0.5 mL), DMSO (0.5 mL), 60 °C. [b]Isolated yield.

clean reaction was observed. The 1,4-substituted triazole **6a** was the single product and could be isolated in 99% yield (Table 3, entry 1). Then the catalyst loading was decreased to 1 mol %, and the yield also decreased to 71% (entry 2). Then another two Cu(I)-MOF catalysts, **1** and **2**, were also examined, and to our delight, they are much more reactive; the target product was isolated in 99% yield within 4 h (entries 3 and 4).

To compare the catalytic activities of these three catalysts, a detailed kinetic study was also conducted (Figure 5a). The

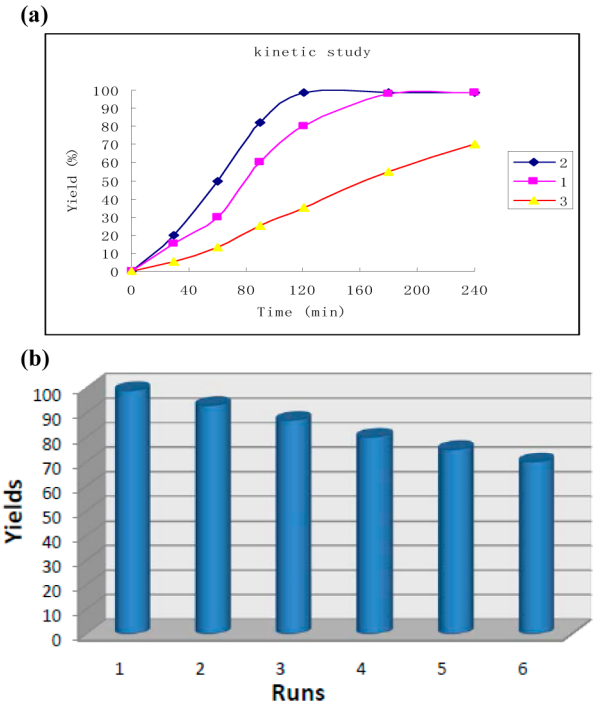

Figure 5. (a) Kinetic study of the three catalytic reactions. One mol % catalyst was used, and ^{1}H NMR yields were recorded by using 1,3,5-trimethoxylbenzene as an internal standard. (b) Recycling experiments for catalyst **2**.

reaction was preformed with 1 mol % catalyst loading, and the yield was determined by ^{1}H NMR by using 1,3,5-trimethoxylbenzene as an internal standard. It was found that the activity order of the three catalysts is **2** > **1** > **3**. The catalyst **2** showed the highest activity in this reaction, and 99% yield was achieved within 2 h. This catalysis activity order is consistent with the fact that (i) **2** has the highest porosity and largest pore diameter (for **1**–**3**, porosity: 25.7%, 29.4%, and 17.6%; pore diameter:

DOI: 10.1021/acs.inorgchem.5b00110
Inorg. Chem. 2015, 54, 4737–4743

2.41, 3.40, and 2.44 Å Supporting Information, Figure S5) and (ii) the labile-coordinated CH_3CN in **2** could be replaced by more active alkynes substrate very easily, giving it more catalytically active Cu(I) sites. Catalysis tests combined with structural analysis demonstrate that the larger porosity and more active metal sites in MOFs could endow the more excellent catalytic performance such as high yield and high reaction rate.

A series of experiments including hot filtration test and inductively coupled plasma (ICP) analysis was performed to verify whether the catalysis of **1**−**3** is really heterogeneous or caused by some leached copper species in the mixtures. For **1**−**3**, when the catalytic reaction was stopped after 1 h, the supernatant was obtained by centrifugation. Almost no further transformation was observed when subjected to standard conditions for another 1 h (for details, Scheme S1 in Supporting Information). ICP analysis of the supernatants gave only trace of residual Cu ions (∼0.007% for **1**, ∼0.003% for **2**, and ∼0.005% for **3**), which may be from some unknown copper species or nanoparticles hard to be removed by filtration. These results clearly demonstrate that the azide−alkyne cycloaddition reaction majorly occurred in the heterogeneity fashion. However, the contribution from leached active species in the solution cannot be ruled out at current stage.

The solids of **1**−**3** could be easily isolated from the reaction suspension by a simple filtration alone and washed thoroughly with dichloromethane. The PXRD experiments of the recovered catalyst show that the integrity of catalyst structure was maintained, and no obvious collapse or decomposition was observed (Supporting Information, Figure S1). For **2**, the recycling experiments presented in Figure 5b suggest a slight decrease in activity from 99% to 87% during the first three cycles. Even after six runs, the yield is still 70%, and when this reaction was extended 8 h longer, the yield increased to 85%.

By using the solid catalyst **2**, the scope of this cycloaddition of various terminal alkynes and various azides was widely investigated (Table 4). The reaction shows a very general substrate scope for different alkynes and azides. Both aliphatic and aromatic alkynes worked very well, and all of the reactions were completed within 4 h in the presence of only 1 mol % catalyst loading. Substrates bearing electron-donating group such as methyl group or electron-withdrawing group at the para position of the phenyl ring are all suitable substrates, providing the corresponding products 95% and 99% yields, respectively (**6b**, **6c**). Functional groups such as cyano group, hydroxy, phenol, and ferrocene are all tolerated in this reaction. The phenyl azide also reacted efficiently with ferrocene acetylene to furnish the functionalized trizazole **6f** in 99% yield.

Table 4. Substrate Scope of Cu(I)-MOF Catalyzed Azide−Alkyne Cycloaddition Reaction[a]

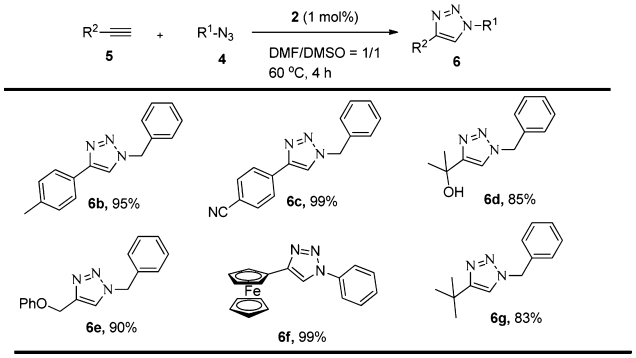

[a]Reaction conditions: benzyl azide **4** (1 mmol), **5** (1 mmol), Cu(I)-MOF catalyst (1 mol %), DMF (0.5 mL), DMSO (0.5 mL), 60 °C, isolated yield.

CONCLUSIONS

In conclusion, we engineered three anion-dependent Cu(I) coordination networks that involved in situ generated cyanide group from the cleavage of a carbon−carbon bond of acetonitrile molecule. The three complexes show diverse structures ranging from 1D ladder (**1**), 3D (3,9)-connected **gfy** network incorporating novel planar $[Cu_3Br]$ triangle (**2**), to 4-connected **sra** network (**3**). They demonstrate good catalytic activity in click reactions. Among them, complex **2** gave the best catalysis performance, which was ascribed to the largest solvent-accessible void and the more potential Cu(I) active sites. The anion-dependent structure assembly, catalytic behavior, and recyclable use of the catalysts have been thoroughly explored, which paves the way for achieving excellent catalysis through tuning of the porosity and potential active metal sites.

ASSOCIATED CONTENT

Supporting Information

Crystal data in CIF files, selected bond lengths and angles in **1**−**3**, IR spectra, TGA data, and powder X-ray diffractograms for **1**−**3**. CCDC 1010017−1010019. The Supporting Information is available free of charge on the ACS Publications website at DOI: 10.1021/acs.inorgchem.5b00110.

AUTHOR INFORMATION

Corresponding Author

*E-mail: dsun@sdu.edu.cn.

Notes

The authors declare no competing financial interest.

ACKNOWLEDGMENTS

This work was supported by the NSFC (Grant No. 21201110), the Special Funding of China Postdoctoral Science Foundation (2013T60663), Research Award Fund for Outstanding Middle-aged and Young Scientist of Shandong Province (BS2013CL010).

REFERENCES

(1) (a) O'Keeffe, M.; Yaghi, O. M. *Chem. Rev.* **2012**, *112*, 675−702. (b) Li, J.-R.; Sculley, J.; Zhou, H.-C. *Chem. Rev.* **2012**, *112*, 869−932. (c) Farha, O. K.; Yazaydin, A. O.; Eryazici, I.; Malliakas, C. D.; Hauser, B. G.; Kanatzidis, M. G.; Nguyen, S. T.; Snurr, R. Q.; Hupp, J. T. *Nat. Chem.* **2010**, *2*, 944−948. (d) Zhang, J.-P.; Zhang, Y.-B.; Lin, J.-B.; Chen, X.-M. *Chem. Rev.* **2012**, *112*, 1001−1033. (e) Hupp, J. T. *Nat. Chem.* **2010**, *2*, 432−433. (f) Wang, C.; Zhang, T.; Lin, W.-B. *Chem. Rev.* **2012**, *112*, 1084−1104. (g) Lee, C.; Farha, O. K.; Roberts, J.; Scheidt, K. A.; Nguyen, S. T.; Hupp, J. T. *Chem. Soc. Rev.* **2009**, *38*, 1450−1459. (h) Wilmer, C. E.; Leaf, M.; Lee, C.; Farha, O. K.; Hauser, B. G.; Hupp, J. T.; Snurr, R. Q. *Nat. Chem.* **2012**, *4*, 83−89. (i) Liu, J.; Chen, L.; Cui, H.; Zhang, J.; Zhang, L.; Su, C.-Y. *Chem. Soc. Rev.* **2014**, *43*, 6011−6061. (j) Corma, A.; García, H.; Llabrés i Xamena, F. X. *Chem. Rev.* **2010**, *110*, 4606−4655.

(2) (a) Campos-Fernández, C. S.; Clérac, R.; Dunbar, K. R. *Angew. Chem., Int. Ed.* **1999**, *38*, 3477−3479. (b) Yuan, G.; Zhu, C.; Liu, Y.; Xuan, W.; Cui, Y. *J. Am. Chem. Soc.* **2009**, *131*, 10452−10460. (c) Lin, Z.; Wragg, D. S.; Warren, J. E.; Morris, R. E. *J. Am. Chem. Soc.* **2007**,

DOI: 10.1021/acs.inorgchem.5b00110
Inorg. Chem. 2015, 54, 4737−4743

129, 10334−10335. (d) Withersby, M. A.; Blake, A. J.; Champness, N. R.; Hubberstey, P.; Li, W. S.; Schroder, M. *Angew. Chem., Int. Ed.* **1997**, *36*, 2327−2329. (e) Campos-Fernández, C. S.; Clérac, R.; Koomen, J. M.; Rusell, D. H.; Dunbar, K. R. *J. Am. Chem. Soc.* **2001**, *123*, 773−774. (f) Lin, J. G.; Xu, Y. Y.; Qiu, L.; Zang, S. Q.; Lu, C. S.; Duan, C. Y.; Li, Y. Z.; Gao, S.; Meng, Q. J. *Chem. Commun.* **2008**, 2659−2661. (g) Lee, E.; Kim, J. Y.; Lee, S. S.; Park, K. M. *Chem.—Eur. J.* **2013**, *19*, 13638−13645. (h) Bu, X. H.; Chen, W.; Hou, W. F.; Du, M.; Zhang, R. H.; Brisse, F. *Inorg. Chem.* **2002**, *41*, 3477−3482.

(3) (a) Chen, Q. H.; Jiang, F. L.; Chen, L.; Yang, M.; Hong, M. C. *Chem.—Eur. J.* **2012**, *18*, 9117−9124. (b) Liu, D.; Lang, J. P.; Abrahams, B. F. *Chem. Commun.* **2013**, *49*, 2682−2684. (c) Chen, X. M.; Tong, M. L. *Acc. Chem. Res.* **2007**, *40*, 162−170. (d) Zhang, X. M. *Coord. Chem. Rev.* **2005**, *249*, 1201−1219.

(4) Li, L.-L.; Liu, L.-L.; Ren, Z.-G.; Li, H.-X.; Zhang, Y.; Lang, J.-P. *CrystEngComm* **2009**, *11*, 2751−2756.

(5) (a) Li, D.; Wu, T.; Zhou, X. P.; Zhou, R.; Hitang, X. C. *Angew. Chem., Int. Ed.* **2005**, *44*, 4175−4178. (b) Guo, L.-R.; Bao, S.-S.; Li, Y.-Z.; Zheng, L.-M. *Chem. Commun.* **2009**, 2893−2895. (c) Zhang, X.-M.; Zhao, Y.-T.; Zhang, W.-X.; Chen, X.-M. *Adv. Mater.* **2007**, *19*, 2843−2846. (d) Deng, H.; Qiu, Y.; Daiguebonne, C.; Kerbellec, N.; Guillou, O.; Zeller, M.; Batten, S. R. *Inorg. Chem.* **2008**, *47*, 5866−5872.

(6) (a) Falkowski, J. M.; Wang, C.; Liu, S.; Lin, W. B. *Angew. Chem., Int. Ed.* **2011**, *50*, 8674−8678. (b) Feng, D. W.; Gu, Z. Y.; Li, J. R.; Jiang, H. L.; Wei, Z. W.; Zhou, H. C. *Angew. Chem., Int. Ed.* **2012**, *51*, 10307−10310. (c) Katz, M. J.; Mondloch, J. E.; Totten, R. K.; Park, J. K.; Nguyen, S. T.; Farha, O. K.; Hupp, J. T. *Angew. Chem., Int. Ed.* **2014**, *53*, 497−501. (d) Nepal, B.; Das, S. *Angew. Chem., Int. Ed.* **2013**, *52*, 7224−7227. (e) Zhao, M. T.; Deng, K.; He, L. C.; Liu, Y.; Li, G. D.; Zhao, H. J.; Tang, Z. Y. *J. Am. Chem. Soc.* **2014**, *136*, 1738−1741. (f) Dhakshinamoorthy, A.; Alvaro, M.; Garcia, H. *Chem.—Eur. J.* **2010**, *16*, 8530−8536. (g) Wang, C.; Wang, J. L.; Lin, W. B. *J. Am. Chem. Soc.* **2012**, *134*, 19895−19908. (h) Song, J.; Luo, Z.; Britt, D. K.; Furukawa, H.; Yaghi, O. M.; Hardcastle, K. I.; Hill, C. L. *J. Am. Chem. Soc.* **2011**, *133*, 16839−16846. (i) Genna, D. T.; Wong-Foy, A. G.; Matzger, A. J.; Sanford, M. S. *J. Am. Chem. Soc.* **2013**, *135*, 10586−10589. (j) Nguyen, H. G. T.; Schweitzer, N. M.; Chang, C.-Y.; Drake, T. L.; So, M. C.; Stair, P. C.; Farha, O. K.; Hupp, J. T.; Nguyen, S. T. *ACS Catal.* **2014**, *4*, 2496−2500. (k) Lalonde, M. B.; Farha, O. K.; Scheidt, K. A.; Hupp, J. T. *ACS Catal.* **2012**, *2*, 1550−1554. (l) Kozachuk, O.; Luz, I.; Llabres i Xamena, F. X.; Noei, H.; Kauer, M.; Albada, H. B.; Bloch, E. D.; Marler, B.; Wang, Y.; Muhler, M.; Fischer, R. A. *Angew. Chem., Int. Ed.* **2014**, *53*, 7058−7062. (m) Liu, Y.; Xi, X.; Ye, C.; Gong, T.; Yang, Z.; Cui, Y. *Angew. Chem., Int. Ed.* **2014**, *53*, 13821−13825. (n) Meng, L.; Cheng, Q.; Kim, C.; Gao, W.-Y.; Wojtas, L.; Chen, Y.-S.; Zaworotko, M. J.; Zhang, X. P.; Ma, S. *Angew. Chem., Int. Ed.* **2012**, *51*, 10082−10085.

(7) (a) Feng, D. W.; Gu, Z. Y.; Li, J. R.; Jiang, H. L.; Wei, Z. W.; Zhou, H. C. *Angew. Chem., Int. Ed.* **2012**, *51*, 10307−10310. (b) Sha, S.; Yang, H.; Li, J.; Zhuang, C. F.; Gao, S.; Liu, S. X. *Catal. Commun.* **2014**, *43*, 146−150. (c) Corma, A.; Iglesias, M.; Xamena, F.; Sanchez, F. *Chem.—Eur. J.* **2010**, *16*, 9789−9795. (d) Dhakshinamoorthy, A.; Alvaro, M.; Garcia, H. *Chem.—Eur. J.* **2010**, *16*, 8530−8536. (e) Harding, J. L.; Reynolds, M. M. *J. Am. Chem. Soc.* **2012**, *134*, 3330−3333. (f) Mo, K.; Yang, Y. H.; Cui, Y. *J. Am. Chem. Soc.* **2014**, *136*, 1746−1749. (g) Pullen, S.; Fei, H. H.; Orthaber, A.; Cohen, S. M.; Ott, S. *J. Am. Chem. Soc.* **2013**, *135*, 16997−17003. (h) Roberts, J. M.; Fini, B. M.; Sarjeant, A. A.; Farha, O. K.; Hupp, J. T.; Scheidt, K. A. *J. Am. Chem. Soc.* **2012**, *134*, 3334−3337. (i) Goswami, S.; Jena, H. S.; Konar, S. *Inorg. Chem.* **2014**, *53*, 7071−7073. (j) Yang, T.; Cui, H.; Zhang, C.; Zhang, L.; Su, C.-Y. *Inorg. Chem.* **2013**, *52*, 9053−9059. (k) Falkowski, J. M.; Sawano, T.; Zhang, T.; Tsun, G.; Chen, Y.; Lockard, J. V.; Lin, W. *J. Am. Chem. Soc.* **2014**, *136*, 5213−5216. (l) Bloch, W. M.; Burgun, A.; Coghlan, C. J.; Lee, R.; Coote, M. L.; Doonan, C. J.; Sumby, C. J. *Nat. Chem.* **2014**, *6*, 906−912.

(8) Rostovtsev, V. V.; Green, L. G.; Fokin, V. V.; Sharpless, K. B. *Angew. Chem., Int. Ed.* **2002**, *41*, 2596−2599.

(9) (a) Meldal, M.; Tornoe, C. W. *Chem. Rev.* **2008**, *108*, 2952−3015. (b) Hein, J. E.; Fokin, V. V. *Chem. Soc. Rev.* **2010**, *39*, 1302−1315. (c) Rodionov, V. O.; Presolski, S. I.; Diaz, D. D.; Fokin, V. V.; Finn, M. G. *J. Am. Chem. Soc.* **2007**, *129*, 12705−12712. (d) Kamata, K.; Nakagawa, Y.; Yamaguchi, K.; Mizuno, N. *J. Am. Chem. Soc.* **2008**, *130*, 15304−15310.

(10) (a) Tabares, L. C.; Navarro, J. A. R.; Salas, J. M. *J. Am. Chem. Soc.* **2001**, *123*, 383−387. (b) Llabrés i Xamena, F. X.; Corma, A. *J. Catal.* **2010**, *276*, 134−140.

(11) Siemsen, P.; Livingston, R. C.; Diederich, F. *Angew. Chem., Int. Ed.* **2000**, *39*, 2632−2657.

(12) (a) Blake, A. J.; Champness, N. R.; Hubberstey, P.; Li, W.-S.; Withersby, M. A.; Schroder, M. *Coord. Chem. Rev.* **1999**, *183*, 117−138. (b) Moulton, B.; Zaworotko, M. J. *Chem. Rev.* **2001**, *101*, 1629−1658. (c) Janiak, C. *Dalton Trans.* **2003**, 2781−2804. (d) Biradha, K.; Su, C.-Y.; Vittal, J. J. *Cryst. Growth Des.* **2011**, *11*, 875−886. (e) O'Keeffe, M. *Chem. Soc. Rev.* **2009**, *38*, 1215−1217.

(13) Yang, L.; Powell, D. R.; Houser, R. P. *Dalton Trans.* **2007**, 955−964.

(14) (a) Ley, A. N.; Dunaway, L. E.; Brewster, T. P.; Dembo, M. D.; Harris, T. D.; Baril-Robert, F.; Li, X.; Patterson, H. H.; Pike, R. D. *Chem. Commun.* **2010**, *46*, 4565−4567. (b) Hou, J. Z.; Li, M.; Li, Z.; Zhan, S. Z.; Huang, X. C.; Li, D. *Angew. Chem., Int. Ed.* **2008**, *47*, 1711−1714. (c) Wang, J. H.; Li, M.; Li, D. *Chem. Sci.* **2013**, *4*, 1793−1801.

(15) (a) Blatov, V. A. *TOPOS, A Multipurpose Crystallochemical Analysis with the Package;* Samara State University: Russia, 2004. (b) Blatov, V. A. *Struct. Chem.* **2012**, *23*, 955−963. TOPOS software is available for download at http://www.topos.samsu.ru.

(16) (a) Du, L.; Wang, K.-M.; Fang, R.-B.; Zhao, Q.-H. *Z. Anorg. Allg. Chem.* **2009**, *635*, 375−378. (b) Zhang, X.-M.; Zheng, Y.-Z.; Li, C.-R.; Zhang, W.-X.; Chen, X.-M. *Cryst. Growth Des.* **2007**, *7*, 980−983. (c) Jia, J.; Lin, X.; Wilson, C.; Blake, A. J.; Champness, N. R.; Hubbersty, P.; Walker, G.; Cussen, E. J.; Schröder, M. *Chem. Commun.* **2007**, 840−842.

(17) (a) Volkringer, C.; Popov, D.; Loiseau, T.; Guillou, N.; Férey, G.; Haouas, M.; Taulelle, F.; Mellot-Draznieks, C.; Burghammer, M.; Riekel, C. *Nat. Mater.* **2007**, *6*, 760−764. (b) Wang, F.; Wu, X.-Y.; Yu, R.-M.; Lu, C.-Z. *Inorg. Chem. Commun.* **2012**, *17*, 169−172.

(18) (a) Allen, F. H. *Acta Crystallogr., Sect. B: Struct. Sci.* **2002**, *58*, 380−388. (b) Cambridge Structure Database search, CSD Version 5.35 (Feb 2014).

(19) (a) Sun, J.; Sun, D.; Yuan, S.; Tian, D. X.; Zhang, L. L.; Wang, X. P.; Sun, D. F. *Chem.—Eur. J.* **2012**, *18*, 16525−16530. (b) Bao, X.; Liu, W.; Liu, J. L.; Gomez-Coca, S.; Ruiz, E.; Tong, M. L. *Inorg. Chem.* **2013**, *52*, 1099−1107. (c) Guillet, G. L.; Sloane, F. T.; Ermert, D. M.; Calkins, M. W.; Peprah, M. K.; Knowles, E. S.; Cizmar, E.; Abboud, K. A.; Meisel, M. W.; Murray, L. J. *Chem. Commun.* **2013**, *49*, 6635−6637.

(20) Frisch, M. J.; Trucks, G. W.; Schlegel, H. B. et al. *Gaussian*software; Gaussian, Inc.: Pittsburgh, PA, 2003.

(21) Glendening, E. D.; Reed, A. E.; Carpenter, J. E.; Weinhold, F. *NBO,* Version 3.1; University of Wisconsin, 2013.

(22) (a) Kolb, H. C.; Finn, M. G.; Sharpless, K. B. *Angew. Chem., Int. Ed.* **2001**, *40*, 2004−2021. (b) Moses, J. E.; Moorhouse, A. D. *Chem. Soc. Rev.* **2007**, *36*, 1249−1262. (c) Bock, V. D.; Hiemstra, H.; van Maarseveen, J. H. *Eur. J. Org. Chem.* **2006**, 51−68. (d) Binder, W. H.; Sachsenhofer, R. *Macromol. Rapid Commun.* **2007**, *28*, 15−54.

(23) Monguchi, Y.; Nozaki, K.; Maejima, T.; Shimoda, Y.; Sawama, Y.; Kitamura, Y.; Kitade, Y.; Sajiki, H. *Green Chem.* **2013**, *15*, 490−495.

(24) (a) Farrusseng, D.; Aguado, S.; Pinel, C. *Angew. Chem., Int. Ed.* **2009**, *48*, 7502−7513. (b) Kang, Y.; Wang, F.; Zhang, J.; Bu, X. *J. Am. Chem. Soc.* **2012**, *134*, 17881−17884. (c) He, Q. T.; Li, X. P.; Chen, L. F.; Zhang, L.; Wang, W.; Su, C. Y. *ACS Catal.* **2013**, *3*, 1−9. (d) Yang, T.; Cui, H.; Zhang, C. H.; Zhang, L.; Su, C. Y. *ChemCatChem* **2013**, *5*, 3131−3138. (e) Garcia-Garcia, P.; Muller, M.; Corma, A. *Chem. Sci.* **2014**, *5*, 2979−3007. (f) Dhakshinamoorthy, A.; Garcia, H. *Chem. Soc. Rev.* **2014**, *43*, 5750−5765. (g) Li, P.; Regati, S.; Huang, H.; Arman, H. D.; Zhao, J. C. G.; Chen, B. *Inorg. Chem. Front.* **2015**, *2*, 42−46.

DOI: 10.1021/acs.inorgchem.5b00110
Inorg. Chem. 2015, 54, 4737−4743